mTORC1 activity is dispensable for synthesis of KSHV lytic proteins

Eric S. Pringle[1,2], Carolyn-Ann Robinson[1], Nicolas Crapoulet[3], Andrea L-A. Monjo[1], Andrew M. Leidal[4], Stephen M. Lewis[1,2,3,5,6], Daniel Gaston[2,6], James Uniacke[8], Craig McCormick[1,2*]

[1]Department of Microbiology and Immunology, Dalhousie University, 5850 College Street, Halifax NS, Canada B3H 4R2

[2]Beatrice Hunter Cancer Research Institute, 5850 College Street, Halifax NS B3H 4R2

[3]Atlantic Cancer Research Institute, 35 Providence Street, Moncton NB, Canada E1C 8X3

[4]Department of Pathology, 513 Parnassus Ave., University of California San Francisco, San Francisco CA, USA 94143

[5]Department of Chemistry and Biochemistry, Université de Moncton, Moncton NB, Canada, E1A 3E9

[6]Department of Biology, University of New Brunswick, Saint John NB, Canada, E2L 4L5

[7]Department of Pathology, Dalhousie University, 5850 University Ave., Halifax NS, Canada B3H 1V8

[8]Department of Pathology and Laboratory Medicine, 5788 University Ave., Nova Scotia Health Authority. Halifax NS, Canada B3H 1V8

[9]Department of Molecular and Cellular Biology, University of Guelph, 50 Stone Rd. E., Guelph ON, Canada N1G 2W1

[*]Corresponding author: C.M., craig.mccormick@dal.ca

Running Title: mTORC1-independent synthesis of KSHV proteins

Keywords: KSHV; lytic; mTORC1; eIF4F; translation initiation; polysomes; translational efficiency

Abstract

Herpesvirus genomes are decoded by host RNA polymerase enzymes, generating mRNAs that are post-transcriptionally modified and exported to the cytoplasm through the combined work of host and viral factors. These viral mRNAs bear 5′-m^{7}G caps and poly(A) tails that should permit assembly of canonical eIF4F cap-binding complexes to initiate protein synthesis. However, the precise mechanisms of translation initiation remain to be investigated for most herpesviruses. eIF4F assembly requires mTORC1-dependent phosphorylation of 4E-BP1, which releases eIF4E from repressive protein complexes. Here, we report that mTORC1 is active and eIF4F is readily detectable throughout the Kaposi's sarcoma-associated herpesvirus (KSHV) replication cycle. Pharmacologic inhibition of mTORC1 activity caused eIF4F disassembly in KSHV-infected cells, indicating that the mTORC1/4E-BP1/eIF4F signalling axis was intact during virus replication. mTORC1 activity contributed to global protein synthesis in infected cells and was required for lytic gene expression immediately upon reactivation from latency. However, once early gene expression had begun, mTORC1 activity was largely dispensable for viral genome replication, late gene expression, and release of infectious viral progeny. Furthermore, polysome fractionation and RNA-sequencing analysis demonstrated that the translational efficiency of viral mRNA was unaltered by changes in the abundance of eIF4F. Accumulating evidence suggests that herpesvirus mRNA translation can be initiated in an eIF4F-independent manner by an alternative mTORC1/4EBP1-resistant initiation complex, thereby facilitating translation of viral mRNA and the production of infectious progeny.

Author summary

All viruses require complex host cell machinery to convert viral mRNAs into proteins. Efficient protein synthesis is required to meet the high anabolic demands of a growing cell. A protein complex known as mechanistic target of rapamycin complex 1 (mTORC1) is a master regulator of protein synthesis. In nutrient-rich conditions, mTORC1 is active and promotes protein synthesis. In nutrient-poor conditions or under stress, mTORC1 is rapidly shut off, and global protein synthesis is arrested. Remarkably, we discovered that synthesis of Kaposi's sarcoma-associated herpesvirus (KSHV) proteins is largely resistant to drugs that inhibit mTORC1, including rapamycin and a more recently developed drug known as Torin. These surprising findings suggest that herpesviruses may employ previously unknown mechanisms to ensure efficient synthesis of viral proteins in situations when canonical translation initiation machinery would be expected to succumb to stress.

Introduction

Kaposi's sarcoma-associated herpesvirus (KSHV) is the infectious cause of Kaposi's sarcoma (KS), primary effusion lymphoma (PEL) and multicentric Castleman's disease [1-3]. Like all herpesviruses, KSHV can establish a quiescent form of infection known as latency in which viral gene expression is severely restricted and the genome is maintained in an episomal form. An essential feature of latency is reversibility, which is required for viral replication and production of viral progeny. Reactivation from latency requires the immediate-early lytic switch protein replication and transcriptional activator (RTA) (ORF50), which initiates an ordered, temporal, cascade of gene expression [4,5]. RTA recruits host cell cofactors like RBPκ to transactivate the promoters of viral early genes required for viral genome replication [6,7]. Viral genome replication licenses the transition to ORF24/ORF31/ORF34-dependent transcription of late genes that encode structural proteins [8-11].

KSHV mRNAs are transcribed by host RNA polymerase II (pol II) and post-transcriptionally modified by host 7-methyl guanosine (m^7G) capping, poly-adenylation, and splicing machinery. Co-transcriptional mRNA splicing is required for recruitment of the human transcription/export (hTREX) complex to host cell mRNAs to stabilize and promote the export of messenger ribonucleoproteins (mRNPs). Most KSHV mRNAs are not spliced and hTREX recruitment is mediated directly by a viral RNA-binding protein (RBP) ORF57, a homologue of HSV-1 ICP27, also known as mRNA transcript accumulation (Mta) [12]. ORF57 RNA-binding determinants and interplay with other components of the host mRNA processing machinery remain poorly defined. In addition to controlling viral mRNA stability and export, ORF57 has also been shown to increase viral mRNA translation by binding directly to a host exon-junction complex protein known as PYM [12].

Viral transcripts must compete with host cell mRNAs for ribosomes and translation initiation factors. Translation initiation of capped-and-polyadenylated mRNA typically requires formation of the eukaryotic initiation factor 4F (eIF4F) complex, which comprises the cap-binding protein eIF4E, RNA-helicase eIF4A, and the large scaffolding protein eIF4G [13,14]. Assembly of eIF4F is regulated by eIF4E-binding proteins, such as 4E-BP1, which prevents association of eIF4E and eIF4G. In nutrient-rich conditions 4E-BP1 is maintained in an inactive form by phosphorylation mediated by the serine/threonine kinase mammalian target of rapamycin complex 1 (mTORC1) [15-17]. mTORC1 integrates nutrient and growth promoting signals to regulate translation. mTORC1 also regulates activation of autophagy by inhibitory phosphorylation of ULK1/2 and Atg13 [18].

mTORC1 activation is a hallmark of KSHV infection; several KSHV gene products have been shown to stimulate or mimic mTORC1 activation (reviewed in [19]) and mTORC1 substrates are phosphorylated in KS lesions [20]. KSHV early lytic gene products K1 and vGPCR activate mTORC1 by stimulating the upstream mTORC1 kinase Akt [21,22]. Moreover, two other viral proteins partially mimic mTORC1 signalling. The viral serine/threonine kinase ORF36 has limited homology to the mTORC1 substrate ribosomal protein S6 kinase 1 beta (RPS6KB1, better known as p70S6K1) and phosphorylates a similar array of substrates [23]. In contrast, ORF45 assembles an activated complex of ERK and RSK that can stimulate phosphorylation of eIF4B and ribosomal protein S6 (S6), which are normally phosphorylated in an mTORC1/p70S6K1 dependent manner [24]. Consistent with the action of these viral gene products, 4E-BP1 is hyper-phosphorylated during KSHV lytic replication and lytic replication is permissive for eIF4F assembly [25]. This suggests that eIF4F is available for translation of viral mRNA during lytic replication.

104 mRNA stability and translation are co-ordinately regulated during times of stress by
105 mTORC1 and stress-sensing eIF2α kinases [16,26]. For example, nutrient deprivation inhibits
106 mTORC1, resulting in dephosphorylation of 4E-BP1, preventing eIF4F assembly, and
107 simultaneously triggers general control nonderepressible-2 (GCN2)-mediated phosphorylation of
108 eIF2α. This prevents the formation of the eukaryotic initiation factor 2 (eIF2)–GTP–Met-
109 tRNAMet^{i} ternary complex required for translation initiation. Moreover, mRNAs with 5′
110 terminal oligo pyrimidine (TOP) or pyrimidine-rich translational element (PRTE) sequences
111 have been shown to be very sensitive to mTORC1 inhibition, although precise the mechanisms
112 remain obscure [27,28]. HCMV infection has been shown to reprogram the translational
113 efficiencies (TEs) of cellular mRNAs [29], suggesting that TE is more than an intrinsic quality of
114 an mRNA sequence, but can be dynamically regulated, likely by RBPs. However, it is unclear
115 whether translation of viral mRNPs is affected by stresses that accompany virus replication.
116 Here we show that mTORC1 activity is required for reactivation from latency, but after
117 early gene expression, mTORC1 is largely dispensable for viral genome replication, late gene
118 expression and virion production. We demonstrate that eIF4F assembles during the KSHV lytic
119 cycle in an mTORC1-dependent manner, but eIF4F loss has no significant effect on viral mRNA
120 translational efficiency. These findings suggest that while eIF4F is available for cap-dependent
121 translation initiation during lytic replication, viral mRNA translation can be initiated by an
122 eIF4F-independent mechanism when eIF4F is limited.
123
124
125
126

Results

mTORC1 is dispensable for KSHV genome replication and synthesis of late proteins

KSHV lytic replication features mTORC1 activation [19,30] but it is not yet known whether mTORC1 activity is required to support viral replication. We tested the requirement for mTORC1 activity in the iSLK.219 cell line [31], which displays stable latent KSHV infection and provides the immediate-early (IE) *RTA* gene in *trans* under the control of a doxycycline (dox)-regulated promoter; dox addition causes accumulation of the RTA lytic switch protein and reactivation from latency. Early viral proteins were readily detected at 24h post-lytic induction (hpi; Fig 1A), and genome replication and late gene expression were detected at 48 hpi (Fig 1B-D). Treatment of cells with the herpesvirus DNA polymerase inhibitor phosphonoacetic acid (PAA) at 24 hpi prevented genome replication (Fig 1B) and late protein accumulation (Fig 1A) indicating that only IE and early (E) gene expression occurred by 24 hpi. During lytic replication, iSLK.219 cells express an RFP reporter transgene driven by an RTA-responsive lytic promoter in the viral genome [32]. Without the addition of additional chemical reagents such as phorbol esters (TPA/PMA) or histone deacetylase inhibitors [31], lytic reactivation in iSLK.219 cells is relatively inefficient with only ~20% of cells expressing RFP (Fig 1D).

We used rapamycin and Torin to pharmacologically inhibit mTORC1 and DMSO as a vehicle control in this study. Rapamycin is a relatively inefficient mTORC1 allosteric inhibitor that does not target mTORC2 [33-35]. In iSLK.219 cells, rapamycin treatment delivered at the time of lytic reactivation with dox (0 hpi), inhibited phosphorylation of the downstream mTOR target S6 but had little effect on the phosphorylation status of 4E-BP1 (Fig 1A). In contrast, treatment with the mTOR active site inhibitor Torin, which inhibits both mTORC1 and mTORC2 complexes [34], completely inhibited both S6 and 4E-BP1 phosphorylation. Treatment

150 with rapamycin at the time of dox-induced lytic reactivation (0 hpi) modestly inhibited viral
151 protein accumulation, whereas Torin potently inhibited accumulation of viral proteins across all
152 temporal classes, including IE (RTA), early (E: ORF45) and late (L: K8.1, ORF65) (Fig 1A). In
153 keeping with this broad inhibition of viral protein accumulation, Torin treatment also inhibited
154 accumulation of the RTA-dependent RFP reporter (Fig 1D), newly-replicated viral genomes (Fig
155 1B), and late viral mRNAs (Fig 1C) when delivered concurrently with dox. If treatment with
156 Torin or rapamycin was delayed to 24 hpi, the phosphorylation status of S6 and 4E-BP1 was
157 similar to that of the treatment at 0 hpi, suggesting that mTORC1 is similarly required for
158 phosphorylation of these canonical target proteins throughout lytic replication. However,
159 delaying treatment with Torin to 24 hpi allowed viral genomes to replicate, and late mRNAs and
160 viral proteins to accumulate to levels comparable to vehicle-treated controls over the subsequent
161 24-48 h (Fig 1A-D). These findings suggest that even though mTORC1 is active during KSHV
162 lytic replication, it may be dispensable for the synthesis of viral proteins in middle and late
163 stages of the lytic replication cycle.

164 To determine whether mTOR inhibition affects virion production, we used a FACS-based
165 titering assay to detect the release of recombinant virions bearing a *GFP* gene driven by a
166 constitutive EF-1α promoter. Supernatants from iSLK.219 cultures were used to infect a
167 monolayer of recipient 293A. Quantification of GFP-positive cells in this monolayer by FACS
168 revealed that the first virions are produced by dox-treated iSLK.219 cells as early as 48 hpi and
169 virion production was maximal by 96 hpi (Fig 2A). Cells treated with Torin at 0 produced very
170 few infectious virions, as measured by FACS, but delaying Torin treatment to 12 hpi allowed
171 approximately 50% of maximal virion production compared to vehicle control (Fig 2B).
172 Delaying Torin treatment to 24, 48, and 72 hpi allowed for a steady increased in the release of

infectious virions from these cells, such that treatment with Torin at 72 hpi produced nearly as many virions as vehicle control. We corroborated this finding in TRex-BCBL1-RTA cells [36], a modified PEL cell line which also bears a dox-inducible *RTA* transgene. As in the iSLK.219 cells, dox addition to TRex-BCBL1-RTA cells is sufficient to induce lytic reactivation, which proceeds more rapidly than the iSLK.219 cells, with the virions released at 48 hpi as opposed to 96 hpi. Using an assay to detect DNAse-protected KSHV genomes in the cell supernatant by quantitative PCR, we measured very few viral particles in the cell supernatant at 24 hpi, which greatly increased by 48 hpi (Fig 2C). Torin treatment at 0 hpi completely inhibited release of DNase-protected genomes from TRex-BCBL1-RTA cells, but delay of Torin treatment to 24 hpi allowed the assembly and release of approximately 50% as many viral particles as vehicle control-treated cells. These results indicate that, similar to iSLK.219 cells, virion release from TRex-BCBL1-RTA cells was resistant to Torin treatment once virus replication has begun.

We next developed a *de novo* infection model to determine whether Torin resistance during KSHV lytic replication requires prior latent infection. The iSLK.219 cells and TRex-BCBL1-RTA cells work on the basis of a dox-regulated expression of the immediate early gene *RTA*. We previously observed that *de novo* infection of iSLK cells, which contain a dox-regulated *RTA*, can bypass latency and progress to lytic replication (and generate lytic foci) if the cells are first treated with dox to induce *RTA* expression (data not shown). This is similar to a previous report of lytic foci formed by infection of cells with KSHV-lyt, a BAC36-based recombinant virus that constitutively expresses RTA [37]. We induced RTA expression in uninfected monolayers of iSLK cells with dox for 24 hours prior to infecting the cells with rKSHV.219. The inoculum was removed and replaced with fresh media containing dox. Torin or vehicle was then added to the cells either immediately after recovery or at 24 hours after *de novo*

196 infection. At 96 h after infection, cell supernatants were harvested and virions were titered by
197 FACS, as described above. We observed that Torin treatment at either 0 or 24 h following *de*
198 *novo* infection potently inhibited virion release, suggesting a role for latency in setting the stage
199 for mTOR-independent viral lytic replication (Fig 2D).
200
201 **mTOR activity is dispensable for global new protein synthesis during KSHV lytic**
202 **replication**
203 Host shutoff is a feature of KSHV lytic replication whereby global synthesis of host proteins is
204 inhibited, largely by the viral host shutoff endonuclease SOX [38,39]. Host shutoff limits the
205 ability of the host cell to restrict virus infection and may improve access of viral mRNAs to the
206 host protein synthesis machinery. The requirement for mTOR-mediated eIF4F assembly for
207 global protein synthesis during KSHV lytic replication is unknown. To address this directly, we
208 employed the relatively efficient TRex-BCBL1-RTA cell model, and treated cells with dox and
209 TPA to ensure efficient lytic reactivation. At 10 min prior to harvest, 10 μg/mL puromycin was
210 added to these cells to measure new protein synthesis; puromycin resembles charged tyrosyl-
211 tRNA and is incorporated at the carboxy-terminus of nascent polypeptide chains, thereby
212 preventing elongation. As the amount of puromycin incorporation is directly proportional to the
213 quantity of mRNAs undergoing active translation, detection of puromycin by immunoblotting
214 can be used as a proxy for global protein synthesis [40]. We observed the highest puromycin
215 incorporation into newly synthesized proteins in latently infected cells (Fig 3A and 3B, Lane 1);
216 incorporation was reduced by more than 50% by 12 hpi and approximately 90% by 24 hpi,
217 consistent with previous reports of host shutoff during the KSHV lytic cycle [25]. In this assay,
218 sodium arsenite served as a potent positive control for translation inhibition; treatment of cells

with sodium arsenite for 10 min prior to the addition of puromycin (20 min prior to harvest) caused eIF2α phosphorylation and largely ablated puromycin incorporation. There was a comparable loss of global protein synthesis in all sodium arsenite treated cells. Treatment with Torin caused a significant loss of 60% of global protein synthesis during latency (Fig 3A and 3B, lane 2) but did not significantly reduce global protein synthesis during lytic replication at 12 hpi or 24 hpi (Fig 3A and 3B, Lane 5 and 8) beyond the already diminished rate. Importantly, we observed that Torin completely inhibited mTOR-mediated phosphorylation of 4E-BP1 in both latent and lytic cells (Fig 3A and 3B, Lanes 2, 5, and 8), indicating that the residual global protein synthesis in cells experiencing host shutoff is resistant to 4E-binding proteins, which would normally be expected to efficiently suppress cap-dependent translation. Together, these data suggest that there is a reduced dependence on mTORC1 for protein synthesis in lytic cells.

mTOR inhibition does not affect translational efficiency of viral mRNAs

In response to nutrient stress or pharmacologic inhibition, mTORC1 inactivation prevents eIF4F assembly, which would be expected to broadly inhibit cap-dependent protein synthesis; however, studies of mTORC1 inhibitors in cancer cells have shown that the regulation of mRNA translational efficiency (TE) is complex. For example, select mRNAs bearing terminal oligopyrimidine (TOP) sequences [27] or PRTE sequences [28] at their 5′ ends are most sensitive to mTORC1 inhibition, whereas other mRNAs can be more efficiently translated for unknown reasons. We used polysome analysis followed by RNA-Seq, also known as Pol-Seq, to determine whether mTORC1 inhibition affects the TE of viral mRNAs. In these experiments, we reactivated iSLK.219 with dox only in an attempt to limit other stresses on the cell. As mentioned above, under these conditions many of the iSLK.219 cells do not enter lytic

replication and instead do not reactivate or undergo an abortive replication; thus, dox treatment renders a mixed population of lytic and non-lytic cells. We observed that Torin treatment of latent iSLK.219 cells for 2 h prior to harvest resulted in a substantial shift of mRNAs from the well-translated heavy polysomes to the poorly-translated sub-polysomal fractions (Fig 4A), consistent with our previous observations of diminished rates of global protein synthesis in the TRex-BCBL-RTA model (Fig 3A, lane 2). Similarly, by 48 hpi, we observed a substantial decrease in the mRNAs associated with the polysome fractions in lytic cells compared to latently infected cells (Fig 4A), consistent with the actions of SOX [41]. Addition of Torin the 48 hpi population for 2 h prior to harvest resulted in further shift of mRNA to sub-polysomal fractions. We isolated mRNA from the polysomes of 48 hpi cells treated with either Torin or vehicle control for 2 h, and total RNA from these populations from two independent biological replicates, which were subjected to sequencing by Ion Torrent. We mapped reads on a per-transcript basis using the Hg19 build of the human genome concatenated to the KSHV genome from JSC-1 cells; this is the parental virus strain of the rKSHV.219 cell line [31,32] that we manually re-annotated with the transcript information from KSHV2.0 [42]. We assessed TE by simple division of the number of reads isolated from the polysomes compared to the reads found in the total RNA fraction (#reads polysome / #reads total). Consistent with the literature, we observed alterations in TE of cellular mRNAs in the presence of Torin, with populations of mRNAs displaying increased or decreased TE (Fig 4B). We scored the difference in translational efficiencies by using a sliding-window to calculate a Z-score of each detected transcript compared to the surrounding 200 transcripts of similar abundance as measured by count per million (CPM). The ΔTE of the majority of viral mRNAs (~90%) was not inhibited or enhanced by a conservative Z-score of 1 (Fig 4C, Z-score within 1 SD of the mean in blue, Z-score > 1 SD

of the mean in red), suggesting that the translational efficiencies of viral transcripts are not regulated by the mTORC1/4E-BP/eIF4F axis.

We confirmed these findings in the TRex-BCBL1-RTA cell model by assessing the distribution of host and viral mRNAs in the polysomal and sub-polysomal fractions reactivated with 1 μg/mL dox for 24 h. Consistent with our observations in the iSLK.219 model (Fig 4A), we observed that Torin treatment of lytic TRex-BCBL1-RTA cells for 2 h prior to harvest resulted in a moderate shift of global mRNAs from polysomes to the sub-polysomal fractions (Fig 5A). We harvested mRNA from polysome, monosome (80S), and sub-monosome fractions (unbound RNA, 40S, and 60S), and performed RT-qPCR on select mRNAs as an alternative measure of TE. In these conditions we observed a large shift of β-actin mRNA from heavy polysomes to the monosome and sub-monosome fractions (Fig 5B); however, a significant proportion of translating β-actin mRNA remained in the polysome fractions despite Torin treatment. In contrast, Torin treatment caused the TOP-mRNA Rps20 to completely shift from the polysome fractions to monosome and sub-monosome fractions. VEGF-A and IL-6, two cytokines with significant contributions to Kaposi's sarcoma pathogenesis [22,43,44] were abundant in the monosome fraction in both vehicle control and Torin-treated cells. The monosome fraction was long thought to make insignificant contributions to global protein synthesis, but recent ribosomal foot-printing studies have revealed that monosomes contain translationally active mRNAs, especially those with short open reading frames (ORFs), up-stream ORFs, and mRNAs with low initiation rates [45]. Thus, our findings suggest that key pathogenic host cytokines are normally translated in monosomes or light polysomes and Torin treatment does not displace these mRNAs from the monosomes.

Finally, we measured viral mRNAs from three transcriptional classes, latent (LANA), early (ORF57 and ORF45) or late (ORF26, K8.1, ORF65, and K12). With Torin treatment, all classes of viral mRNAs shift from lighter polysomes accumulate in the monosome fraction, but much of the mRNA is retained in the light and heavy polysome fractions, demonstrating that mTORC1 activity is largely dispensable for translation of these viral messages. These data also suggest that monosomes may have a previously unappreciated role in the synthesis of herpesvirus proteins.

mTOR inhibition during lytic replication disrupts eIF4F assembly

mTORC1 primarily regulates translation initiation by preventing assembly of the eIF4F initiation complex. When hypophosphorylated, 4E-BP1 can bind to the eIF4E cap-binding protein, which prevents recruitment of the eIF4G scaffolding protein. mTORC1-mediated phosphorylation of 4E-BP1 enables eIF4F assembly and subsequent recruitment of the eIF3 complex and the small ribosomal subunit [15,16]. mTORC1 activity during KSHV replication was previously shown to enable the assembly of eIF4F [25]. To further examine the role of mTORC1 activity on eIF4F regulation during lytic replication we performed m^7GTP Sepharose bead pull-downs in native lysates from both latent and reactivated iSLK.219 cell and TRex-BCBL1-RTA cell models, and probed for assembly of canonical and alternative eIF4F constituent proteins in the presence or absence of mTORC1 inhibition with Torin. eIF4G1 and eIF4G3 were co-captured on m^7GTP Sepharose beads with eIF4E1 and eIF4E2 cap-binding proteins from latent and lytic iSLK.219 lysates (Fig 6A), suggesting the potential for formation of canonical and non-canonical eIF4F complexes at all stages of viral replication. eIF4G1 and eIF4G3 were depleted from these complexes when cells were treated with Torin for 2 h prior to harvest, while there was a

reciprocal increase in unphosphorylated 4E-BP1 detected in the pulldowns (Fig 6A, lanes 4, 6, 8). Interestingly, we observed a marked increase in binding of eIF4E2 to the m^{7}GTP Sepharose beads as the lytic cycle progressed, but this did not aid recruitment of eIF4G3 in the presence of Torin (Fig 6A, lanes 4-8). Together, these data confirm that eIF4F can indeed be disrupted by mTORC1 inhibition during the lytic cycle.

To investigate the effects of long-term mTORC1 inhibition in this model, we treated lytic iSLK.219 cells with Torin at 24 hpi and harvested lysates for m^{7}GTP Sepharose bead pulldown at 48 hpi. Similar to the 2 h Torin treatments shown in Fig 6A, 24 h of sustained mTORC1 inhibition during lytic replication also impaired eIF4F assembly (Fig 6B), while selectively inhibiting the accumulation of total eIF4G1 and eIF4E2 proteins. We corroborated these findings in the TRex-BCBL1-RTA cell model; treatment of latent or lytic cells with Torin for 2 h prior to lysate harvest completely inhibited eIF4F assembly by allowing unphosphorylated 4E-BP1 to block recruitment of eIF4G1 or eIF4G3 to eIF4E1/eIF4E2 proteins (Fig 6C). It is important to note that there is a limitation to the experiments described in Fig 6; as the bait is an analogue of the mRNA cap, the m^{7}GTP Sepharose bead pulldown assay should only detect free eIF4F complexes that are not already bound to mRNA in the lysate. Thus, it is possible that viral mRNPs retain intact eIF4F in these lysates, making them exempt from regulation by 4E-BP1; however, long-term Torin treatments shown in Fig 1 and Fig 2, which began during early replication and proceeded to late replication, permitted efficient synthesis of viral late proteins and release of infectious virions, respectively. Taken together, these data suggest that in Torin-treated lytic cells the translation of late viral mRNAs is efficiently initiated and translated under conditions where eIF4F is depleted. This suggests that either viral mRNAs can efficiently

scavenge the remaining residual pool of eIF4F in the cell, or that initiation of these transcripts can be accomplished independently of intact eIF4F.

mTORC1 inhibition alters the composition of mRNPs in polysomes

We assessed the protein composition of mRNPs in polysomes in latent or lytic TRex-BCBL-RTA cells by immunoblotting for proteins harvested from several polysome fractions. We elected to use a low-salt lysis buffer in these experiments to aid retention of eIF4F components and other RNA binding proteins, consistent with previous ribosome isolation protocols [46,47]. We isolated fractions containing the 40S, 60S, and 80S sub-polysomal peaks, as well as light and heavy polysomes. RNA and associated proteins were precipitated using ethanol and a glycogen co-precipitant. We found that the m^7GTP cap-binding proteins eIF4E1, eIF4E2, and NCBP80 were associated with polysomes in all conditions tested (Fig 7). Inhibition of mTORC1 with Torin leads to a progressive loss of eIF4F components eIF4G1 and eIF4G3 from polysomal fractions, consistent with the displacement of eIF4G from the eIF4F complex by hypophosphorylated 4E-BP1. However, eIF4G2, which was found primarily in the 80S monosome peak and sub-monosomal fractions, was unaffected by mTORC1 inhibition. eIF4G2 does not contain an N-terminal domain required for association with eIF4E1 and is thought to be involved in cap-independent translation mechanisms [48,49]. We noted a clear accumulation of a faster migrating species of eIF4G1 that matches a previously reported caspase-3 cleavage fragment [50] consistent with induction of apoptosis in this population of cells [51]. Hyper-phosphorylated 4E-BP1 was associated with polysomes in vehicle-treated samples, consistent with other reports of 4E-binding proteins co-sedimenting with polysome fractions [52]. Hypophosphorylated 4E-BP1 was found in sub-polysomal fractions of Torin-treated cells in both

355 the latent and lytic cell populations. We interpret this finding as dynamic disassembly of eIF4F
356 on mRNA in polysomes allowing opportunistic binding of 4E-BP1 to eIF4E [14]. Finally,
357 consistent with previous reports [12], we observed ORF57 association with mRNPs in
358 polysomes, which was impervious to mTORC1 inhibition. Taken together, these findings
359 indicate that mTORC1 is active during lytic replication and eIF4F is assembled, but also that
360 synthesis of viral proteins has a limited requirement for eIF4F, and there is remodelling of
361 polysome- and monosome-associated mRNP complexes during lytic replication.
362

363 ## Discussion

364 The seminal discovery that rapamycin (aka sirolimus) treatment causes regression of iatrogenic
365 Kaposi's sarcoma (KS) lesions suggests a central role for mTORC1 in KSHV biology [20].
366 mTORC1 activity has since been shown to be required for pro-inflammatory signalling in KS
367 models [22,43,44]. Here we directly assessed the role of mTORC1 and the eIF4F complex in the
368 translation of KSHV mRNA. mTORC1was required for reactivation from latency, consistent
369 with previous findings that rapamycin treatment caused diminished RTA transcript and protein
370 accumulation in the BCBL-1 PEL cell line [53]; however, once early replication was established
371 in these cells the requirement for mTORC1 was greatly reduced, as genome replication and
372 virion production proceeded normally when mTORC1 is inhibited by Torin. Importantly, we
373 demonstrated that late viral mRNA can accumulate normally (Fig 1C) and can be initiated for
374 translation (Fig 4, 5B) when Torin is applied during early replication. Furthermore, these late
375 transcripts are efficiently translated despite being first transcribed under conditions where eIF4F
376 is disassembled and unavailable (Fig 6B, 7), and generate sufficient protein to produce infectious

377 virions (Fig 1B, 2). This suggests that while mTORC1 is active during lytic replication, it is
378 dispensable for translation of viral mRNA.

379 During lytic replication we observed a change in global protein synthesis consistent with
380 host-shutoff and the need for viruses to prioritize translation of viral mRNA during infection. We
381 found that mTORC1 inhibition in the low-translation lytic environment had minimal effect on
382 the overall translational output of the cell (Figs. 3, 4A). The loss of ~60% of global protein
383 synthesis with Torin treatment of latently infected cells is consistent with other studies in
384 uninfected cells [27,28]. It is becoming clear that the remaining mTORC1-independent protein
385 synthesis in these systems involves non-eIF4F initiation systems. Recently, N^6-methyladenosine
386 (m^6A) dependent translation initiation has been shown to contribute to residual translation
387 following eIF4F disassembly in normoxia [54], whereas during hypoxia eIF4E2 and eIF4G3
388 form an alternative eIF4F complex required for nearly all translation [55,56]; however, we
389 observed a clear loss of eIF4G3 from polysomes following Torin treatment (Fig 7), suggesting
390 that KSHV is probably not co-opting alternative hypoxic translation initiation complexes.
391 Several studies have reported m^6A modification of KSHV mRNAs, and m^6A modification of
392 RTA is required for proper splicing [57-59]; however, for the most part precise roles for m^6A
393 modifications and m^6A reader proteins in the biogenesis and fate of KSHV mRNAs remain to be
394 discovered, and may be dependent on cell type and different chemical stimuli of lytic
395 reactivation [57].

396 mRNA translational efficiency is governed by *cis*-acting sequences and RNA-binding
397 proteins. For example, ribosomal proteins are strongly down-regulated by mTORC1 inhibition,
398 consistent with our observations shown in Figure 5B, due to both loss of eIF4F-dependent
399 initiation and binding of LARP1 to a 5'-m^7G-cap-proximal TOP sequence [27,60-62]. We note

that the identified transcription start-sites for KSHV mRNAs generally lack TOP or PRTE sequences, which suggests that their translation might not be especially susceptible to mTORC1 inhibition. In our experiments, Torin treatments caused a global change in translational efficiencies (Fig 4), but the TE of viral transcripts remained similar to vehicle control, demonstrating that mTORC1 is not required for efficient synthesis of viral proteins. These observations are consistent with reports from Lenarcic, et. al. (2014), who demonstrated that mTORC1 is dispensable for HCMV late protein synthesis and that TE of viral mRNAs was minimally affected by Torin [63]. Together, these reports suggest that resistance to eIF4F loss might be a general feature of herpesvirus translation, even for viruses like HCMV that do not shut off host gene expression.

Our Pol-Seq analysis was restricted to actively-translating heavy polysomes, but light polysomes and monosomes also make important contributions to global protein synthesis [45]. We extended and confirmed our Pol-Seq data by measuring the distribution of pathogenic cytokines and a panel of viral transcripts. For many of the viral transcripts, we observed a consistent distribution in the heaviest polysome fractions (fractions 9 and 10), and thereby most translationally active, irrespective of Torin treatment. Viral transcripts were also observed to shift from the light fractions to the lighter monosome fractions in response to Torin but did not sediment in sub-polysomal fractions. We were surprised to see abundant IL-6 and VEGFA mRNAs accumulate in the monosome fraction with little material present in the heavy polysome fractions. Monosomes are enriched for short transcripts (ORF length < 590 nt) and IL-6 approaches this limit (639 nt CDS, Accession NM_000600.4) [44]. IL-6 contains several upstream start codons, but does not appear to encode any uORFs. VEGFA is twice the length of average ORFs found in monosomes (1239 nt CDS, Accession NM_001025366.2), but its

translation is regulated by a complex arrangement of two internal-ribosomal entry sites, near-cognate start codons, and uORFs, likely accounting for its inefficient initiation (reviewed in [64]).

Inhibition of mTORC1 during lytic replication leads to disassembly of eIF4G from the cap-binding eIF4E (Figs. 6, 7). We could observe this disassembly both in a cap-analogue pulldown experiments (Fig 6) and through displacement of eIF4G1 and eIF4G3 from lytic polysomes without loss of cap-binding proteins (eIF4E1, eIF4E2, NCBP) and no change in eIF4G2, a homologue of eIF4G that lacks the N-terminal eIF4E binding domain (Fig 7). Our data is consistent with destabilization of eIF4G association with eIF4E on cap binding and dynamic disassembly of eIF4F after initiation, as hypothesized by Merrick, 2015 [14]. eIF4E appears to remain associated with the cap of the polysomal mRNA, allowing a surface for interaction with either eIF4G, or a 4E-BP1 protein that would prevent additional eIF4G association and subsequent rounds of eIF4F-dependent initiation. We hypothesize that the presence of hyper-phosphorylated 4E-BP1 in vehicle-treated polysomes is due to low affinity binding of 4E-BP1 to the eIF4E; high affinity binding of hypo-phosphorylated 4E-BP causes rapid loss of initiation on these mRNAs and their subsequent shift to sub-polysomal fractions. KSHV lytic proteins have been shown to activate mTORC1, which should promote assembly of eIF4F by displacing 4E-BP1. However, the rapid disassembly of free eIF4F and displacement of eIF4G from polysomes upon Torin treatment during all stages of KSHV infection suggests that KSHV gene products only enforce eIF4F-dependent translation upstream of mTORC1 and have no downstream mechanism to sustain eIF4F assembly.

During Torin treatment, both the TOP-containing transcript Rps20 and the non-TOP β-actin transcript were depleted from polysome fractions that retained viral mRNAs (Fig 5B). In

these same fractions eIF4G1 and eIFG3 are also lost, but ORF57 is retained. ORF57 and related herpesvirus homologues (EBV EB2, HSV1/2 ICP27) have previously been shown to interact with translation initiation factors, and could be found in polysomes [65,66]. Ectopically expressed ORF57 co-immunoprecipitates with 48S components [12] and co-sediments in polysomes without viral mRNA present (unpublished observations). Both EB2 and ICP27 associate with PABP, which can further recruit eIF4G. This is likely responsible for the phenomena of 3′UTR tethering of ICP27 and EB2 and enhanced translation of reporter luciferase mRNA in *in vitro* assays [67,68]. Tethering ICP27 is also sufficient to promote translation of uncapped, non-polyadenylated RNA [69]. Ectopic expression of ORF57, EB2, or ICP27 do not globally enhance protein synthesis, but they do enhance translation of non-spliced RNA, partially through enhanced mRNA nuclear export [70]. In our experiments, loss of eIF4G from polysomes upon Torin treatment suggests that ORF57-dependent recruitment of eIF4G to viral mRNAs is not required for their translation, yet ORF57 is clearly present in the same fractions as viral mRNA and is not displaced with eIF4F loss. It is possible that other KSHV proteins may associate with polysomes. Other groups have made important progress in this area by identifying several viral proteins using an oligo-dT purification of HCMV-infected cells followed by LC-MS/MS [71]. Their approach used high-salt washes for increased stringency; however, as high-salt can dissociate canonical translation initiation factors, there remains the likelihood that more viral RNA-binding proteins remain to be identified.

If mTORC1 is active during lytic replication and is not required for translation of viral mRNA, then why is it active? mTORC1-dependent phosphorylation impacts many cellular processes and any of these could require regulation by the virus. In our virus titering experiments, we observed production of infectious virions following Torin treatment, but to a

lesser extent than the vehicle control. If translation of viral mRNAs is not inhibited, it is possible that eIF4F-dependent translation of cellular proteins is required for optimal virus replication or for spread *in vivo*. Our experiments also take place at normal atmospheric oxygen levels, whereas in the human host KSHV resides and replicates in compartments with a lower oxygen tension. Under these physiological oxygen conditions, eIF4E1- and eIF4E2-dependent translation are both active [72]. Enforcing eIF4E1-dependent translation under these circumstances might be important for replication. mTORC1 inhibition activates autophagy through loss of ULK1 phosphorylation at Ser757 [73]. Suppression of mTORC1 by Torin treatment could lead to induction of autophagy in our system and reduce accumulation of infectious virions. At least three KSHV proteins modulate autophagy, vFLIP, K7, and vBcl2 (reviewed in [74]), suggesting that autophagy is an important regulator of virus infection. Activation of mTORC1 by vGPCR, K1, and ORF45 might also suppress autophagy induction. mTORC1 activity could also be important for KSHV to maintain "normal" contacts with other immune cells or for the production of cytokines during establishment of latency. Gammaherpesvirus latency in distinct niches of the B cell compartment requires emulation or stimulation of a germinal centre reaction [75]. Rapamycin was recently shown to inhibit normal germinal centre reactions [76,77]. Together, these findings suggest that mTORC1 activity may be required for proper establishment of the latently infected B cell compartment *in vivo*. Given the lack of immunocompetent animal models for KSHV, the role of mTORC1 for establishing gammaherpesvirus latency might best be elucidated in murine gammaherpesvirus 68 models of infection.

Here, our data suggests that while mTORC1 is active during KSHV lytic replication and is likely important for the virus life cycle, it is not required for the translation of viral mRNA. More

generally, during lytic replication the global protein synthesis remaining is resistant to eIF4F disassembly. This suggests that viral transcripts can access alternative translation initiation machinery during lytic replication. Whether this machinery is accessed from the host translation repertoire or encoded within the viral genome remains to be determined.

Materials and Methods

Cell lines

HEK293A (293A) (ATCC), and iSLK and iSLK.219 cells (a gift from Don Ganem [31]) were cultured in DMEM with 10% heat-inactivated FBS with 100 IU of each penicillin and streptomycin. Trex-BCBL1-RTA cells (a gift from Jae Jung [36]) were cultured in RPMI-1640 supplemented with 10% heat-inactivated FBS, 500 µM ß-mercaptoethanol, with 100 IU of each penicillin and streptomycin. All cells were maintained at 37°C with 5% CO_2 atmosphere. Cells were regularly assessed for mycoplasma DAPI staining and fluorescent microscopy. iSLK.219 cells were cultured in the presence of 10 µg/mL of puromycin (Invitrogen) to maintain copy number of the episomal rKSHV.219 genomes [31,32]. Puromycin was not included in the media of cells seeded for experiments. iSLK.219 cells were diluted to a density of 10^5 cells/mL for seeding in all experiments. To induce RTA transgene expression in iSLK.219 cells, on the day following seeding medium was refreshed and supplemented with 1 µg/mL doxycycline (dox, Sigma). Trex-BCBL1-RTA cells were resuspended at a density of $2.5x10^5$ cells/mL supplemented with 1 µg/mL dox or 1 µg/mL dox with 20 ng/mL 12-O-Tetradecanoylphorbol-13-acetate (TPA, Sigma) to induce RTA transgene expression.

Chemical inhibitors

Torin 1, referred to as "Torin" here, (Toronto Research Chemicals) [34] and Rapamycin (Sigma) were resuspended in DMSO, which was used as a vehicle control in all experiments at 0.1% v/v. Rapamycin and Torin were both used at a concentration of 250 nM. Phosphonoacetic acid and arsenic oxide were purchased from Sigma. Phosphonoacetic acid was used at a concentration of 500 μM.

Fluorescent imaging and counting

iSLK.219 cells were seeded in a 6-well plate and fixed with 4% paraformaldehyde for 15 minutes at room temperature and the nuclei were stained with Hoechst 33342 (Invitrogen). Fluorescent images were captured using an EVOS FL Cell Imaging System (ThermoFisher) and RFP+ cells and Hoechst+ cells were counted using a custom CellProfiler ver 3.0.0 script [78].

Immunoblotting

Cells were washed with ice-cold PBS and harvested in 2x Laemmli Buffer. The protein concentration of whole cell lysates was quantified by DC protein assay (Bio-Rad) and equal quantities of protein were loaded for SDS-PAGE and transferred to PVDF membranes (Bio-Rad). For proteins isolated from pulldowns or precipitated form polysome fractions, equal volumes of lysate were loaded. Membranes were blocked with 5% skim milk-Tris-buffered-saline-0.1% Tween (ThermoFisher) (TBS-T), or 5% bovine serum albumin (BSA) TBS-T, and probed at 4^{o}C overnight with the following primary antibodies: S6 (Cell Signaling; #2217), pS6 (Ser235/236, Cell Signaling #4858), Puromycin (clone 12D10, EMD Millipore; MABE343MB), eIF2alpha (Cell Signaling; #9722), phospho-eIF2alpha (Ser51, Cell Signaling; #3597), 4E-BP1 (Cell Signaling; #9644), eIF4E (Cell Signaling; #2067), eIF4G1 (Cell Signaling; #2858), eIF4G3

(GeneTex; GTX118109), eIF4E2 (GeneTex; GTX103977), NCBP80 (Abcam), β-actin (Cell Signaling; #5125), RTA (a kind gift from David Lukac), ORF45 (Thermo-Fisher; MA5-14769), ORF57 (Santa Cruz; sc135746), K8.1 (clone 4A4, ABI; 13-212-100), LANA (a kind gift from Don Ganem), and ORF65 (a kind gift from Jae Jung). Primary antibody was detected with horseradish-peroxidase conjugated anti-mouse (Cell Signaling; #7076) and anti-rabbit (Cell Signaling; #7074) secondary antibodies. Blots were developed with Clarity-ECL chemiluminescence reagent (Bio-Rad) and imaged on a Bio-Rad Chemidoc-Touch.

Viral genome amplification and qRT-PCR

DNA was harvested from the cells using QIAamp DNA Mini Kit (Qiagen) as per the manufacturers' directions. qPCR was performed with primers to ORF26 and β-actin GoTaq qPCR Master Mix (Promega). KSHV genome copy number is represented as fold excess of ORF26 over β-actin. For qRT-PCR, total RNA was extracted using the RNeasy Plus Kit extraction (Qiagen), reverse transcribed using MaximaH (ThermoFisher) using random hexamers for priming as per the manufactures' directions. qPCR was performed using GoTaq. Both adherent and non-adherent cells were harvested in each sample. Transcripts were normalized to abundance of 18S rRNA using the **ΔΔ**Cq method. Primer sequences are in listed in S2 Table 2.

DNAse-protected virion qPCR

At the time of harvest, the cells and debris were pelleted for 5 min at 5000 x g. 180 µL of the supernatant was treated with 300 µg/mL DNase I (Sigma), for 30 min at 37°C. DNA was then extracted from the treated supernatant using DNeasy Blood and Tissue Minikit (Qiagen) as per the manufacturers' instructions with the following modifications: lysis buffer AL was

supplemented with 10 mg/sample of salmon sperm DNA (Invitrogen) and 1 ng of the luciferase (*luc2*) containing plasmid, pGL4.26 (Clontech). qPCR was performed with primers for ORF26 to detect viral genomes and the *luc* carrier plasmid using Go-Taq (Promega). ORF26 quantity was normalized to *luc2* using the **ΔΔ**Cq method.

KSHV infection and titering

rKSHV.219 contains an EGFP cassette under a constitutive EF1α promoter, allowing for quantification by flow cytometry [32]. Supernatant was harvested from iSLK.219 cells as indicated and stored at -80^{o}C until titering. One day prior to titering, 2.5x10^{5} 293A cells were plated in each well of a 12 well plate. The thawed viral inoculum was mixed by inversion then centrifuged at 5000 x g for 5 min to pellet debris. The cells were then infected with diluted inoculum and centrifuged at 800 x g for 90-120 min [80]. Immediately after spinoculation, the inoculum was removed, the cells were washed once with PBS, and fresh media was added, and the cells were returned to an incubator. The day following infection, 293A cells were lifted with trypsin, washed once in cold PBS then resuspended in 1% paraformaldehyde PBS. GFP+ cells were recorded from 10 000 events in an arbitrary live FSC/SSC gate with a FACScalibur (BD Bioscience). Data was analysed using Flowing Software ver 2.5 (Perttu Terho, Turku Centre for Biotechnology, Finland. www.flowingsoftware.com).

Puromycin Translation Assay

TRex-BCBL1-RTA cells were treated with 10 µg/mL puromycin for 10 min prior to harvest in 2x Laemmli buffer. C-terminal puromycin was probed by western blot using an anti-puromycin antibody [40]. Western blots were performed on 4-15% Mini-PROTEAN TGX Stain-Free

584 gradient gels (Bio-Rad) as per the manufacturers' instructions. The Stain-Free total protein
585 loading control was used to quantify the anti-puromycin signal.
586
587 **m^{7}GTP pull-down**
588 2x10^6 iSLK, iSLK.219 cells, or 5x10^6 TRex-BCBL1-RTA cells were used for each pull-down.
589 After treatment with Torin or DMSO, cells were washed twice with ice-cold PBS and harvested.
590 The cells were centrifuged for 5 min at 1000 x g and the pellet was lysed, on ice for 10 min in
591 lysis buffer (20 mM Tris-HCl, 150 mM, NaCl, 0.5% NP-40 with protease and phosphatase
592 inhibitors). The lysates were centrifuged for 5 min at 10 000 g and the supernatant were pre-
593 cleared with 30 µL settled volume of unconjugated agarose beads (Jena Biosciences, Germany)
594 by incubating with end-over-end rotation, for 10 min at 4^{o}C. The beads were pelleted by
595 centrifugation for 30 s at 500 x g and 50 µL of supernatant was removed as the 5% input control.
596 The remaining supernatant was incubated with m^{7}GTP agarose beads (Jena Biosciences,
597 Germany) for 4-6 h at 4^{o}C, with agitation. The beads were washed four times with lysis buffer.
598 The beads were then resuspended in 50 µL of 1x Laemmli buffer with 100 mM DTT and boiled
599 at 55^{o}C for 10 min.
600
601 **Polysome analysis**
602 Polysomes were isolated by ultracentrifugation of cytosolic lysate through a 7-47% linear
603 sucrose gradient in high salt (20 mM Tris HCl, 300 mM NaCl, 25 mM $MgCl_2$ in DEPC-treated
604 or nuclease-free water, Fig 4 and 5) or low salt (15 mM Tris HCl, 50 mM KCl, 10 mM $MgCl_2$
605 Fig 7) lysis buffer with RNAse and protease inhibitors. High salt conditions were used to isolate
606 RNA from gradients and low salt conditions were used for isolating proteins. Gradients were

prepared using manufactures' settings on a Gradient Master 108 (Biocomp). For each gradient, ~8 x 10^6 iSLK.219 or 1.3 x 10^7 TRex-BCBL-RTA cells were seeded. Cells were treated with 100 µg/mL cycloheximide (CHX, Acros Organics or Sigma) for 3 min prior to harvest. Adherent and detached cells were washed and collected in ice-cold PBS. The cells were pelleted by centrifugation for 5 min at 500 x g and washed again with ice-cold PBS. Cell pellets were resuspended in lysis buffer (high or low salt buffer, with 1% Triton X-100, 400 U/ml RNAseOUT (Invitrogen), 100 µg/mL CHX, and protease and phosphatase inhibitors) for 10 min on ice. Lysate was centrifuged for 10 min at 2 300 x g, the supernatant were transferred to a new tube and centrifuged for 10 min at 15 000 x g. The supernatant was overlaid on the sucrose gradients. Gradients were centrifuged at 39 000 rpm for 90 min on a SW-41 rotor. The bottom of the centrifuge tube was punctured and the gradient was underlaid with 60% sucrose by syringe pump to collect 1 mL fractions from the top of the gradient with simultaneous A_{260} measurement using a UA-6 detector (Brandel, MD). Polysome sedimentation graphs were generated with GraphPad Prism.

RNA-Seq analysis of polysome fractions

Total RNA or pooled fractions from heavy polysomes were isolated using Ribozol (Amresco) using standard procedures, except the precipitant in the aqueous fraction was isolated using an RNeasy column (QIAGEN). mRNA was isolated from these total fractions using polyA enrichment (Dynabeads mRNA DIRECT Micro Purification Kit, ThermoFisher) according to the manufacturers' protocol, then library preparation was performed with Ion Total RNA-Seq Kit v2.0 (ThermoFisher). Library size, concentration, and quality was assessed using a 2200 TapeStation (Agilent). Libraries were sequenced on Proton sequencer (ThermoFisher Scientific)

with a PI chip and the Ion PI Hi-Q Sequencing 200 Kit for 520 flows. Ion Torrent reads were processed using combined Human Hg19 and KSHV (Accession GQ994935) reference transcriptomes. The KSHV genome was manually re-annotated with the transcript definitions from KSHV2.0 [42] reference transcriptome and the Quasi-Mapping software Salmon [80]. Normalized counts per million (cpm) were estimated for individual transcripts using the R package limma [81]. Two biological replicates were combined as a geometric mean [82]. The transcripts were ordered by abundance and the mean, standard deviation (SD), and Z-score were calculated using a sliding window of 200 transcripts of similar abundance [82,83]. The most abundant 100 and the least abundant 100 transcripts used the mean and SD of the adjacent bin. Translational efficiency (TE) of a transcript treatment was determined by the formula TE = $\log_2$(polysome/total). The change in translational efficiency (ΔTE) = TE_{Torin}-TE_{DMSO}.

Polysome qRT-PCR

Trex-BCBL1-RTA were reactivated with 1 µg/mL dox for 24h. Torin or DMSO was added 2 h prior to harvest in high salt lysis buffer as described above. Fractions were mixed 1:1 with Trizol and isolated as per manufacturers' directions with the following exceptions: 30-60 µg of GlycoBlue Co-Precipitant (Ambion) and 100 ng of *in vitro* transcribed luciferase DNA (NEB T7 HiScribe) were added to the aqueous fractions during isopropanol precipitation. The resulting pellet was resuspended in nuclease-free water and reverse transcribed with MaximaH using random primers. mRNA was normalized to luciferase spike to control for recovery. The quantity of mRNA detected in a given fraction was then calculated as a percentage of the total detected in all fractions. The RNA recovery was controlled by subtracting the Cq of the luciferase spike, which was assumed to be constant, from the target Cq: $\Delta Cq = Cq_{target} - Cq_{luc}$. This ΔCt value for

653 each fraction was then subtracted from the lightest fraction: $\Delta\Delta Cq_n=\Delta Cq_1-\Delta Cq_n$ where
654 n=fraction number. ΔΔCt was then normalized into a transcript quantity, $Q_n=2^{\Delta\Delta Cqn}$ for each
655 transcript. The total quantity transcript (Q_{total}) was summed from all fractions:
656 $Q_{total}=Q_1+Q_2+Q_3+\ldots+Q_n$ and the proportion (P) of a transcript found in a fraction was
657 determined by $P=Q_n/Q_{total}$ [84].
658
659 **Polysome immunoblot**
660 500 µL fractions of sucrose gradient were mixed with 45 µg of GlycoBlue and 1.5 mL of 100%
661 ethanol and incubated overnight at -80°C. Fractions were centrifuged at 15 000 x g for 15 min at
662 4°C. Supernatants were decanted and the pellets were washed with 70% ethanol. Residual
663 ethanol was air dried at 95°C and the pellet was resuspended in 1x Laemmli buffer with 100 mM
664 DTT then boiled at 95°C for 5 min prior to analysis by SDS-PAGE.
665
666 **Statistical analysis**
667 We used Prism7 (GraphPad) to perform statistical analysis. Unpaired Student's t-tests were used
668 to compare two groups. Two-way ANOVA was used compare between multiple groups with a
669 post-hoc test to determine differences between groups. p-value <0.05 were considered significant
670 and indicated with (*).
671
672 ## Supporting Information
673 **Table S1. Pol-Seq data**. (.xlsx) Transcript abundances in cpm and calculated TE are provided
674 and Z-scores are provided. Raw data are deposited in NCBI.
675 **Table S2. Oligonucleotide sequences used in this study.** (.xlsx)

Acknowledgements

We thank members of the McCormick lab for critical reading of this manuscript. We would like to thank Don Ganem (Novartis), Jae Jung (USC), and David Lukac (Rutgers) for providing reagents.

Figure Legends

Fig 1. mTOR is required for reactivation from latency, but not progression from early to late replication. (A) iSLK.219 cells were treated with 1 μg/mL doxycycline (dox) to induce lytic reactivation and harvested with 2x Laemmli buffer as indicated. DMSO, Torin, Rapamycin or phosphonoacetic acid (PAA) was added either at 0 or 24 hpi. Samples were probed by western blot as indicated. (B) Left. DNA was extracted from iSLK.219 cells at indicated times and the relative proportion of KSHV genome to human genomic DNA was determined by comparing the proportion of ORF26 to β-actin by qPCR.n=3 ± SEM. Right. DNA was harvested from iSLK.219 cells at 72 hpi. Cells were treated as indicated at either 0 or 24 hpi. n=3 ± SEM. (C). As in (B) except RNA was extracted and qRT-PCR performed for the late genes ORF26 and K8.1. n=4 ± SEM. (D) iSLK.219 cells were treated with dox to induce lytic reactivation and treated with Torin or DMSO at 0 or 24 hpi. Cells were fixed with 4% paraformaldehyde and nuclei were stained with Hoechst. RFP+ cells and nuclei were imaged on an inverted fluorescent microscope and enumerated with CellProfiler. n=3 ± SD. * indicates p value < 0.05 by t-test or one-way ANOVA.

Fig 2. mTOR is not required for production of infectious virions after KSHV reactivation. (A) iSLK.219 cells were reactivated with dox. Cell supernatants were harvested at the times

699 indicated at stored at -80°C before further processing. Supernatants were cleared of debris by
700 centrifugation (5000 x g) and used to infect monolayers of 293A cells. 24 h after infection, 293A
701 cells were resuspended with trypsin and fixed with 1% paraformaldehyde. GFP+ cells from an
702 arbitrary live-dead gate were recorded by flow cytometry. n=4, ±SEM. (B) As in (A) except
703 Torin was DMSO were added to the media at the indicated times post reactivation. Supernatants
704 were harvested at 96 hpi and titered as described in (A). (C) TRex-BCBL1-RTA cells were
705 reactivated with 1 μg/mL dox. Torin or DMSO was added to the cells at 0 or 24 hpi. At 48 hpi,
706 cells and debris were removed by centrifugation (5000 x g) and supernatants were stored at -
707 80°C. Supernatants were treated with DNase I for 30 min at 37°C before DNA harvest in lysis
708 buffer containing a salmon sperm carrier DNA and a luciferase-encoding plasmid. DNAse-
709 protected viral genomes were quantified with qPCR using luciferase DNA as a recovery control.
710 n=5 ±SEM. (D). Uninfected iSLK cells were treated with 1 μg/mL dox for 24 h to induce RTA
711 expression. These cells were infected with KSHV derived from iSLK.219 for 2 h. After
712 infection, media was replaced with dox-containing media. Torin or DMSO was added to the
713 refreshed wells at the end of infection or 24 h post-infection. 96 h post-infection, supernatant was
714 removed and titered by infecting 293A as described in (A). n=4 ±SEM. * indicates p value <
715 0.05 by t-test or one-way ANOVA.
716
717 **Fig 3. Protein synthesis remaining after virus host shutoff is resistant to further mTOR**
718 **inhibition.** (A) Trex-BCBL1-RTA cells were reactivated from latency with 1 μg/mL dox and 20
719 ng/mL TPA. Cells were treated with Torin or DMSO for 2 h prior to harvest or with sodium
720 arsenite for 20 min prior to harvest. All cells were pulsed with 10 μg/mL puromycin 10 min prior
721 to harvest in 2x Laemmli buffer. Lysates were probed by western blot using antibodies as

722 indicated. Incorporation of puromycin in nascent polypeptide chains indicates the rate or protein
723 synthesis as detected by probing with an anti-puromycin antibody. (B) The puromycin intensity
724 in A was quantified and compared to the total protein load as described in Methods. Intensities
725 were normalized to the latent, DMSO-treated cells (Lane 1). Lane numbers correspond to lanes
726 reading left to right in A. n=4, ± SD. * indicates p value < 0.05 by one-way ANOVA.
727
728
729 **Fig 4. Effect of Torin treatment on translational efficiencies of viral mRNA.** (A) Polysome
730 profiles of latent or 48 hpi iSLK.219 treated with either Torin or DMSO for 2 h prior to harvest.
731 Cells were treated with 100 µg/mL cycloheximide (CHX) for 5 minutes prior to harvest to
732 prevent elongation. Cells were lysed in the presence of CHX and loaded on a 7-47% linear
733 sucrose gradient. After separation by ultracentrifugation, the abundance of RNA (A_{260} nm) in the
734 gradient was continually measure as fractions were collected. RNA from the 48 hpi polysome
735 fractions was isolated for sequencing. (B) mRNA from translating ribosomes (of DMSO treated
736 cells) was sequenced and aligned to both the human and KSHV genomes. Viral transcripts are
737 depicted in blue on top of the grey background of cellular genes. The dashed line represents the
738 mean TE of all transcripts. (C) The ΔTE of viral transcripts is depicted in blue or read on a grey
739 background of cellular genes. Viral transcripts beyond one SD of the mean are red, viral
740 transcripts within on SD are depicted in blue. Vertical lines represent a 1.5-fold change in
741 transcript TE.
742
743 **Fig 5. Distribution of viral and cellular mRNAs in polysome fractions.** (A) Polysome profile
744 of TRex-BCBL1-RTA cells induced with 1 µg/mL dox for 24 h. Torin or DMSO control were

added 2 h prior to harvest and polysome analysis. (B) qRT-PCR analysis of cellular and viral transcripts in polysome fractions. Total RNA was isolated from polysome fractions. RNA was co-precipitated with GlycoBlue and T7-transcribed luciferase RNA to improve and normalize for recovery. RNA was analysed by qRT-PCR for cellular, and viral transcripts. DMSO – black line, Torin – red line. Vertical lines depict the boundaries between the monosomes, light polysome, and heavy polysome fractions. Polysome fractions are depicted in grey. Mean of three independent biological replicates is shown.

Fig 6. mTOR inhibition disrupts eIF4F formation during latency and lytic replication. (A) Uninfected iSLK cells, iSLK.219 during latency, 24, or 48 hpi were treated for 2h with Torin or DMSO and harvested at the indicated times. Cell lysates were incubated with m^7GTP Sepharose, washed and eluted by boiling in 1x Laemmli buffer and analyzed by western blot. (B) As in (A), except iSLK.219 cells were treated with Torin or DMSO at 24 hpi prior to at 48 hpi harvest. (C) Latent or 24 hpi TRex-BCBL1-RTA cells treated and harvested as in (A).

Fig 7. Association of translation initiation factors during viral latency and lytic replication. (A) TRex-BCBL-RTA cells at 24 hpi were treated with Torin or DMSO for 2 h prior to harvest. The indicated 40S, 60S, 80S, light, and heavy polysome fractions were precipitated with ethanol and glycogen. (B) Precipitate from polysome fractions in (A) were resuspended in 1x Laemmli buffer analysed by western blot as indicated.

768

References

1. Chang Y, Cesarman E, Pessin MS, Lee F, Culpepper J, Knowles DM, et al. Identification of herpesvirus-like DNA sequences in AIDS-associated Kaposi's sarcoma. Science. 1994;266: 1865–1869.

2. Cesarman E, Chang Y, Moore PS, Said JW, Knowles DM. Kaposi's sarcoma-associated herpesvirus-like DNA sequences in AIDS-related body-cavity-based lymphomas. N Engl J Med. 1995;332: 1186–1191. doi:10.1056/NEJM199505043321802

3. Soulier J, Grollet L, Oksenhendler E, Cacoub P, Cazals-Hatem D, Babinet P, et al. Kaposi's sarcoma-associated herpesvirus-like DNA sequences in multicentric Castleman's disease. Blood. 1995;86: 1276–1280.

4. SUN R, Lin SF, Gradoville L, Yuan Y, Zhu F, Miller G. A viral gene that activates lytic cycle expression of Kaposi's sarcoma-associated herpesvirus. Proc Natl Acad Sci USA. 1998;95: 10866–10871.

5. Lukac DM, Renne R, Kirshner JR, Ganem D. Reactivation of Kaposi's sarcoma-associated herpesvirus infection from latency by expression of the ORF 50 transactivator, a homolog of the EBV R protein. Virology. 1998;252: 304–312. doi:10.1006/viro.1998.9486

6. Liang Y, Chang J, Lynch SJ, Lukac DM, Ganem D. The lytic switch protein of KSHV activates gene expression via functional interaction with RBP-Jκ (CSL), the target of the Notch signaling pathway. Genes & Development. 2002;16: 1977–1989. doi:10.1101/gad.996502

7. Izumiya Y, Izumiya C, Hsia D, Ellison TJ, Luciw PA, Kung HJ. NF- κB Serves as a cellular sensor of Kaposi's Sarcoma-Associated Herpesvirus latency and negatively regulates K-Rta by antagonizing the RBP-Jκ coactivator. Journal of Virology. 2009;83: 4435–4446. doi:10.1128/JVI.01999-08

8. Brulois K, Wong L-Y, Lee H-R, Sivadas P, Ensser A, Feng P, et al. Association of Kaposi's Sarcoma-Associated Herpesvirus ORF31 with ORF34 and ORF24 is critical for late gene expression. Journal of Virology. 2015;89: 6148–6154. doi:10.1128/JVI.00272-15

9. Davis ZH, Verschueren E, Jang GM, Kleffman K, Johnson JR, Park J, et al. Global mapping of Herpesvirus-host protein complexes reveals a transcription strategy for late genes. Molecular Cell. 2015;57: 1–12. doi:10.1016/j.molcel.2014.11.026

10. Davis ZH, Hesser CR, Park J, Glaunsinger BA. Interaction between ORF24 and ORF34 in the Kaposi's Sarcoma-Associated Herpesvirus late gene transcription factor complex is essential for viral late gene expression. Journal of Virology. 2015;90: 599–604. doi:10.1128/JVI.02157-15

11. Nishimura M, Watanabe T, Yagi S, Yamanaka T, Fujimuro M. Kaposi’s sarcoma-

associated herpesvirus ORF34 is essential for late gene expression and virus production. Scientific Reports. 2017;7: 1–12. doi:10.1038/s41598-017-00401-7

12. Boyne JR, Jackson BR, Taylor A, Macnab SA, Whitehouse A. Kaposi's sarcoma-associated herpesvirus ORF57 protein interacts with PYM to enhance translation of viral intronless mRNAs. The EMBO Journal. Nature Publishing Group; 2010;29: 1851–1864. doi:10.1038/emboj.2010.77

13. Hinnebusch AG. The scanning mechanism of eukaryotic translation initiation. Annu Rev Biochem. 2014;83: 779–812. doi:10.1146/annurev-biochem-060713-035802

14. Merrick WC. eIF4F: A retrospective. Journal of Biological Chemistry. 2015;290: 24091–24099. doi:10.1074/jbc.R115.675280

15. Glaunsinger BA. Modulation of the translational landscape during Herpesvirus infection. Annual Review of Virology. 2015;2: 311–333. doi:10.1146/annurev-virology-100114-054839

16. Jan E, Mohr I, Walsh D. A cap-to-tail guide to mRNA translation strategies in virus-infected cells. Annual Review of Virology. 2015;3: annurev–virology–100114–055014. doi:10.1146/annurev-virology-100114-055014

17. Siddiqui N, Sonenberg N. Signalling to eIF4E in cancer. Biochemical Society Transactions. 2015;43: 763–772. doi:10.1042/BST20150126

18. Jung CH, Jun CB, Ro S-H, Kim Y-M, Otto NM, Cao J, et al. ULK-Atg13-FIP200 complexes mediate mTOR signaling to the autophagy machinery. Mol Biol Cell. 2009;20: 1992–2003. doi:10.1091/mbc.E08-12-1249

19. Bhatt AP, Damania B. AKTivation of PI3K/AKT/mTOR signaling pathway by KSHV. Front Immunol. 2012;3: 401. doi:10.3389/fimmu.2012.00401

20. Stallone G, Stallone G, Schena A, Schena A, Infante B, Infante B, et al. Sirolimus for Kaposi's sarcoma in renal-transplant recipients. N Engl J Med. 2005;352: 1317–1323. doi:10.1056/NEJMoa042831

21. Zhang Z, Chen W, Sanders MK, Brulois KF, Dittmer DP, Damania B. The K1 protein of Kaposi's Sarcoma-Associated Herpesvirus augments viral lytic replication. Journal of Virology. 2016;90: 7657–7666. doi:10.1128/JVI.03102-15

22. Martin D, Nguyen Q, Molinolo A, Gutkind JS. Accumulation of dephosphorylated 4EBP after mTOR inhibition with rapamycin is sufficient to disrupt paracrine transformation by the KSHV vGPCR oncogene. Oncogene. Nature Publishing Group; 2013;: 1–8. doi:10.1038/onc.2013.193

23. Bhatt AP, Wong JP, Weinberg MS, Host KM, Giffin LC, Buijnink J, et al. A viral kinase mimics S6 kinase to enhance cell proliferation. Proceedings of the National Academy of Sciences. 2016;: 201600587. doi:10.1073/pnas.1600587113

24. Kuang E, Tang Q, Maul GG, Zhu F. Activation of p90 ribosomal S6 kinase by ORF45 of Kaposi's Sarcoma-Associated Herpesvirus and its role in viral lytic replication. Journal of Virology. 2008;82: 1838–1850. doi:10.1128/JVI.02119-07

25. Arias C, Walsh D, Harbell J, Wilson AC, Mohr I. Activation of host translational control pathways by a viral developmental switch. PLoS Pathog. 2009;5: e1000334. doi:10.1371/journal.ppat.1000334.s001

26. Wek RC, Jiang H-Y, Anthony TG. Coping with stress: eIF2 kinases and translational control. Biochemical Society Transactions. 2006;34: 7–11. doi:10.1042/BST20060007

27. Thoreen CC, Chantranupong L, Keys HR, Wang T, Gray NS, Sabatini DM. A unifying model for mTORC1-mediated regulation of mRNA translation. Nature. 2012;486: 109–113. doi:10.1038/nature11083

28. Hsieh AC, Hsieh AC, Liu Y, Liu Y, Edlind MP, Edlind MP, et al. The translational landscape of mTOR signalling steers cancer initiation and metastasis. Nature. Nature Publishing Group; 2012;485: 55–61. doi:10.1038/nature10912

29. McKinney C, Zavadil J, Bianco C, Shiflett L, Brown S, Mohr I. Global reprogrammingof the cellular translational landscape facilitates cytomegalovirus replication. Cell Reports. 2014;6: 9–17. doi:10.1016/j.celrep.2013.11.045

30. Chang HH, Chang HH, Ganem D, Ganem D. A unique herpesviral transcriptional program in KSHV-infected lymphatic endothelial cells leads to mTORC1 activation and rapamycin sensitivity. Cell Host Microbe. 2013;13: 429–440. doi:10.1016/j.chom.2013.03.009

31. Myoung J, Ganem D. Generation of a doxycycline-inducible KSHV producer cell line of endothelial origin: maintenance of tight latency with efficient reactivation upon induction. Journal of Virological Methods. 2011;174: 12–21. doi:10.1016/j.jviromet.2011.03.012

32. Vieira J, O'Hearn PM. Use of the red fluorescent protein as a marker of Kaposi's sarcoma-associated herpesvirus lytic gene expression. Virology. 2004;325: 225–240. doi:10.1016/j.virol.2004.03.049

33. Guertin DA, Sabatini DM. Defining the Role of mTOR in Cancer. Cancer Cell. 2007;12: 9–22. doi:10.1016/j.ccr.2007.05.008

34. Thoreen CC, Kang SA, Chang JW, Liu Q, Zhang J, Gao Y, et al. An ATP-competitive mammalian target of rapamycin inhibitor reveals rapamycin-resistant functions of mTORC1. J Biol Chem. 2009;284: 8023–8032. doi:10.1074/jbc.M900301200

35. Kang SA, Pacold ME, Cervantes CL, Lim D, Lou HJ, Ottina K, et al. mTORC1 Phosphorylation Sites Encode Their Sensitivity to Starvation and Rapamycin. Science. 2013;341: 1236566–1236566. doi:10.1126/science.1236566

36. Nakamura H, Lu M, Gwack Y, Souvlis J, Zeichner SL, Jung JU. Global changes in

Kaposi's Sarcoma-Associated Virus gene expression patterns following expression of a tetracycline-inducible Rta transactivator. Journal of Virology. 2003;77: 4205–4220. doi:10.1128/JVI.77.7.4205-4220.2003

37. Budt M, Hristozova T, Hille G, Berger K, Brune W. Construction of a lytically replicating Kaposi's Sarcoma-Associated Herpesvirus. Journal of Virology. 2011;85: 10415–10420. doi:10.1128/JVI.05071-11

38. Glaunsinger B, Ganem D. Highly selective escape from KSHV-mediated host mRNA shutoff and its implications for viral pathogenesis. Journal of Experimental Medicine. 2004;200: 391–398. doi:10.1182/blood.V97.10.3244

39. Glaunsinger B, Ganem D. Lytic KSHV infection inhibits host gene expression by accelerating global mRNA turnover. Molecular Cell. 2004;13: 713–723.

40. Schmidt EK, Clavarino G, Ceppi M, Pierre P. SUnSET, a nonradioactive method to monitor protein synthesis. Nature Methods. 2009;6: 275–277. doi:10.1038/nmeth.1314

41. Covarrubias S, Gaglia MM, Kumar GR, Wong W, Jackson AO, Glaunsinger BA. Coordinated destruction of cellular messages in translation complexes by the gammaherpesvirus host shutoff factor and the mammalian exonuclease Xrn1. PLoS Pathog. 2011;7: e1002339. doi:10.1371/journal.ppat.1002339.s007

42. Arias C, Weisburd B, Stern-Ginossar N, Mercier A, Madrid AS, Bellare P, et al. KSHV 2.0: a comprehensive annotation of the Kaposi's sarcoma-associated herpesvirus genome using next-generation sequencing reveals novel genomic and functional features. PLoS Pathog. 2014;10: e1003847. doi:10.1371/journal.ppat.1003847

43. Roy D, Roy D, Sin SH, Sin SH, Lucas A, Lucas A, et al. mTOR Inhibitors Block Kaposi Sarcoma Growth by inhibiting essential autocrine growth factors and tumor angiogenesis. Cancer Research. 2013;73: 2235–2246. doi:10.1158/0008-5472.CAN-12-1851

44. Sodhi A, Chaisuparat R, Hu J, Ramsdell AK, Manning BD, Sausville EA, et al. The TSC2/mTOR pathway drives endothelial cell transformation induced by the Kaposi's sarcoma-associated herpesvirus G protein-coupled receptor. Cancer Cell. 2006;10: 133–143. doi:10.1016/j.ccr.2006.05.026

45. Heyer EE, Moore MJ. Redefining the translational status of 80S monosomes. Cell. 2016;164: 757–769. doi:10.1016/j.cell.2016.01.003

46. Mehta P, Woo P, Venkataraman K, Karzai AW. Ribosome purification approaches for studying interactions of regulatory proteins and RNAs with the ribosome. Methods Mol Biol. 2012;905: 273–289. doi:10.1007/978-1-61779-949-5_18

47. Belin S, Hacot S, Daudignon L, Therizols G, Pourpe S, Mertani HC, et al. Purification of ribosomes from human cell lines. Curr Protoc Cell Biol. 2010;Chapter 3: Unit 3.40. doi:10.1002/0471143030.cb0340s49

913 48. Imataka H, Olsen HS, Sonenberg N. A new translational regulator with homology to
914 eukaryotic translation initiation factor 4G. The EMBO Journal. 1997;16: 817–825.
915 doi:10.1093/emboj/16.4.817

916 49. Henis-Korenblit S, Shani G, Sines T, Marash L, Shohat G, Kimchi A. The caspase-
917 cleaved DAP5 protein supports internal ribosome entry site-mediated translation of death
918 proteins. Proc Natl Acad Sci USA. 2002;99: 5400–5405. doi:10.1073/pnas.082102499

919 50. Bushell M, Poncet D, Marissen WE, Flotow H, Lloyd RE, Clemens MJ, et al. Cleavage of
920 polypeptide chain initiation factor eIF4GI during apoptosis in lymphoma cells:
921 characterisation of an internal fragment generated by caspase-3-mediated cleavage. Cell
922 Death Differ. 2000;7: 628–636. doi:10.1038/sj.cdd.4400699

923 51. Tabtieng T, Degterev A, Gaglia MM. Caspase-dependent suppression of type I interferon
924 signaling promotes Kaposi's Sarcoma-Associated Herpesvirus Lytic replication. Journal of
925 Virology. 2018;92. doi:10.1128/JVI.00078-18

926 52. Castelli LM, Talavera D, Kershaw CJ, Mohammad-Qureshi SS, Costello JL, Rowe W, et
927 al. The 4E-BP Caf20p mediates both eIF4E-dependent and independent repression of
928 translation. PLoS Genet. 2015;11: e1005233. doi:10.1371/journal.pgen.1005233.s008

929 53. Nichols LA, Adang LA, Kedes DH. Rapamycin blocks production of KSHV/HHV8:
930 insights into the anti-tumor activity of an immunosuppressant drug. Nichols LA, Adang
931 LA, Kedes DH. PLoS ONE. 2011;6: e14535. doi:10.1371/journal.pone.0014535.g005

932 54. Coots RA, Liu X-M, Mao Y, Dong L, Zhou J, Wan J, et al. A facilitates eIF4F-
933 independent mRNA translation. Molecular Cell. 2017;68: 504–514.e7.
934 doi:10.1016/j.molcel.2017.10.002

935 55. Ho JJD, Wang M, Audas TE, Kwon D, Carlsson SK, Timpano S, et al. Systemic
936 reprogramming of translation efficiencies on oxygen stimulus. Cell Reports. 2016;14:
937 1293–1300. doi:10.1016/j.celrep.2016.01.036

938 56. Uniacke J, Holterman CE, Lachance G, Franovic A, Jacob MD, Fabian MR, et al. An
939 oxygen-regulated switch in the protein synthesis machinery. Nature. 2013;486: 126–129.
940 doi:10.1038/nature11055

941 57. Hesser C, Karijolich J, Dominissini D, He C, Glaunsinger BA. N 6-methyladenosine
942 modification and the YTHDF2 reader protein play cell type specific roles in lytic viral
943 gene expression during Kaposi's sarcoma-associated herpesvirus infection. Plos Pathog.
944 2018;14: e1006995. doi:10.1101/201475

945 58. Ye F, Chen ER, Nilsen TW. Kaposi's Sarcoma-Associated Herpesvirus utilizes and
946 manipulates RNA N 6-Adenosine methylation to promote lytic replication. Journal of
947 Virology. 2018;92: e00220-18. doi:10.1128/JVI.00466-17

948 59. Tan B, Liu H, Zhang S, da Silva SR, Zhang L, Meng J, et al. Viral and cellular N 6-
949 methyladenosin and N 6, 2'-O-dimethyladenosine epitranscriptomes in the KSHV life

cycle. Nature Microbiology. 2017;3: 108–120. doi:10.1038/s41564-017-0056-8

60. Lahr RM, Fonseca BD, Ciotti GE, Al-Ashtal HA, Jia J-J, Niklaus MR, et al. La-related protein 1 (LARP1) binds the mRNA cap, blocking eIF4F assembly on TOP mRNAs. eLife. 2017;6. doi:10.7554/eLife.24146

61. Tcherkezian J, Cargnello M, Romeo Y, Huttlin EL, Lavoie G, Gygi SP, et al. Proteomic analysis of cap-dependent translation identifies LARP1 as a key regulator of 5'TOP mRNA translation. Genes & Development. 2014;28: 357–371. doi:10.1101/gad.231407.113

62. Philippe L, Vasseur J-J, Debart F, Thoreen CC. La-related protein 1 (LARP1) repression of TOP mRNA translation is mediated through its cap-binding domain and controlled by an adjacent regulatory region. Nucleic Acids Research. 2017. doi:10.1093/nar/gkx1237

63. Lenarcic EM, Ziehr B, De Leon G, Mitchell D, Moorman NJ. Differential role for host translation factors in host and viral protein synthesis during human cytomegalovirus infection. Journal of Virology. 2014;88: 1473–1483. doi:10.1128/JVI.02321-13

64. Arcondeguy T, Lacazette E, Millevoi S, Prats H, Touriol C. VEGF-A mRNA processing, stability and translation: a paradigm for intricate regulation of gene expression at the post-transcriptional level. Nucleic Acids Research. 2013;41: 7997–8010. doi:10.1016/j.cell.2011.10.002

65. Ricci EP, Mure F, Gruffat H, Decimo D, Medina-Palazon C, Ohlmann T, et al. Translation of intronless RNAs is strongly stimulated by the Epstein–Barr virus mRNA export factor EB2. Nucleic Acids Research. 2009;37: 4932–4943. doi:10.1128/JVI.02665-06

66. Larralde O, Smith RWP, Wilkie GS, Malik P, Gray NK, Clements JB. Direct stimulation of translation by the multifunctional Herpesvirus ICP27 protein. Journal of Virology. 2006;80: 1588–1591. doi:10.1128/JVI.80.3.1588-1591.2006

67. Smith RWP, Anderson RC, Larralde O, Smith JWS, Gorgoni B, Richardson WA, et al. Viral and cellular mRNA-specific activators harness PABP and eIF4G to promote translation initiation downstream of cap binding. Proceedings of the National Academy of Sciences. 2017;114: 6310–6315. doi:10.1016/S0022-2836(02)00655-1

68. Mure F, Panthu B, Zanella-Cléon I, Delolme F, Manet E, Ohlmann T, et al. Epstein-Barr Virus protein EB2 stimulates translation initiation of mRNAs through direct interactions with both poly(A)-binding protein and eukaryotic initiation factor 4G. Journal of Virology. 2018;92. doi:10.1128/JVI.01917-17

69. Smith RWP, Anderson RC, Larralde O, Smith JWS, Gorgoni B, Richardson WA, et al. Viral and cellular mRNA-specific activators harness PABP and eIF4G to promote translation initiation downstream of cap binding. Proceedings of the National Academy of Sciences. 2017;114: 6310–6315. doi:10.1016/S0022-2836(02)00655-1

70. Sandri-Goldin RM. The many roles of the highly interactive HSV protein ICP27, a key regulator of infection. Future Microbiology. 2011;6: 1261–1277. doi:10.2217/fmb.11.119

71. Lenarcic EM, Ziehr BJ, Moorman NJ. An unbiased proteomics approach to identify human cytomegalovirus RNA-associated proteins. Virology. 2015;481: 13–23. doi:10.1016/j.virol.2015.02.008

72. Timpano S, Uniacke J. Human cells cultured under physiological oxygen utilize two cap-binding proteins to recruit distinct mRNAs for translation. Journal of Biological Chemistry. 2016;: jbc.M116.717363. doi:10.1074/jbc.M116.717363

73. Kim J, Kundu M, Viollet B, Guan K-L. AMPK and mTOR regulate autophagy through direct phosphorylation of Ulk1. Nature Cell Biology. 2011;13: 132–141. doi:10.1038/ncb2152

74. Choi Y, Bowman JW, Jung JU. Autophagy during viral infection— a double-edged sword. Nature Reviews Microbiology. 2018;16: 341–354. doi:10.1038/s41579-018-0003-6

75. Speck SH, Ganem D. Viral latency and its regulation: lessons from the gammaherpesviruses. Cell Host Microbe. 2010;8: 100–115. doi:10.1016/j.chom.2010.06.014

76. Ersching J, Efeyan A, Mesin L, Jacobsen JT, Pasqual G, Grabiner BC, et al. Germinal center selection and affinity maturation require dynamic regulation of mTORC1 kinase. Immunity. 2017;46: 1045–1064.e0. doi:10.1016/j.immuni.2017.06.005

77. Ye L, Lee J, Xu L, Mohammed A-U-R, Li W, Hale JS, et al. mTOR promotes antiviral humoral immunity by differentially regulating CD4 helper T cell and B cell responses. Journal of Virology. 2017;91. doi:10.1128/JVI.01653-16

78. Carpenter AE, Jones TR, Lamprecht MR, Clarke C, Kang IH, Friman O, et al. CellProfiler: image analysis software for identifying and quantifying cell phenotypes. Genome Biol. 2006;7: R100. doi:10.1186/gb-2006-7-10-r100

79. Yoo S-M, Ahn A-K, Seo T, Hong HB, Chung M-A, Jung S-D, et al. Centrifugal enhancement of Kaposi's sarcoma-associated virus infection of human endothelial cells in vitro. Journal of Virological Methods. 2008;154: 160–166. doi:10.1016/j.jviromet.2008.07.026

80. Patro R, Duggal G, Love MI, Irizarry RA, Kingsford C. salmon provides fast andbias-aware quantificationof transcript expression. Nature Methods. 2017;14: 417–419. doi:10.1038/nmeth.4197

81. Ritchie ME, Phipson B, Wu D, Hu Y, Law CW, Shi W, et al. limma powers differential expression analyses for RNA-sequencing and microarray studies. Nucleic Acids Research. 2015;43: e47–e47. doi:10.1186/s13059-014-0465-4

82. Quackenbush J. Microarray data normalization and transformation. Nat Genet. 2002;32: 496–501. doi:10.1038/ng1032

83. Andreev DE, O'Connor PBF, Fahey C, Kenny EM, Terenin IM, Dmitriev SE, et al. Translation of 5' leaders is pervasive in genes resistant to eIF2 repression. eLife. 2015;4: e03971. doi:10.7554/eLife.03971

84. Panda A, Martindale J, Gorospe M. Polysome Fractionation to Analyze mRNA Distribution Profiles. BIO-PROTOCOL. 2017;7. doi:10.21769/BioProtoc.2126

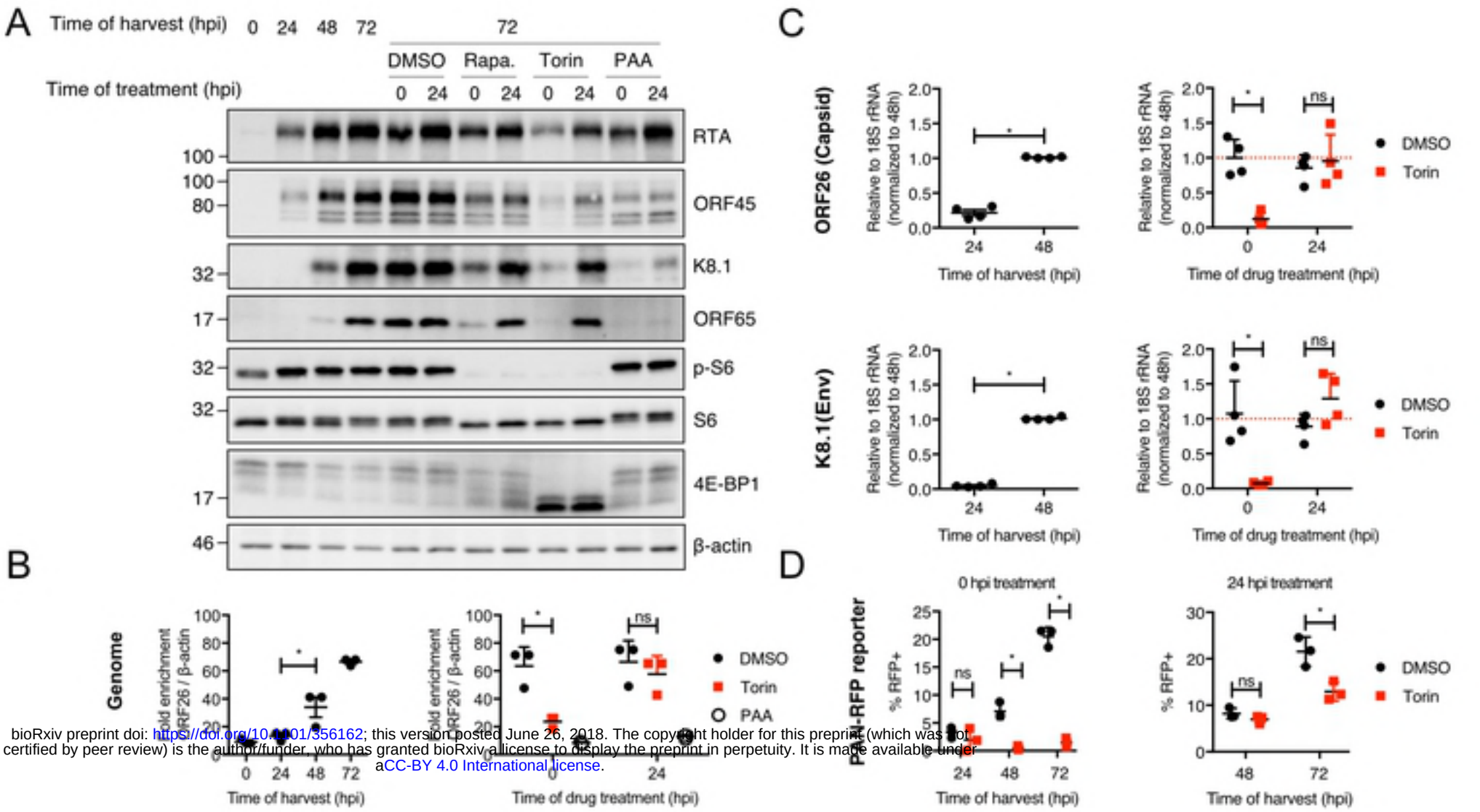

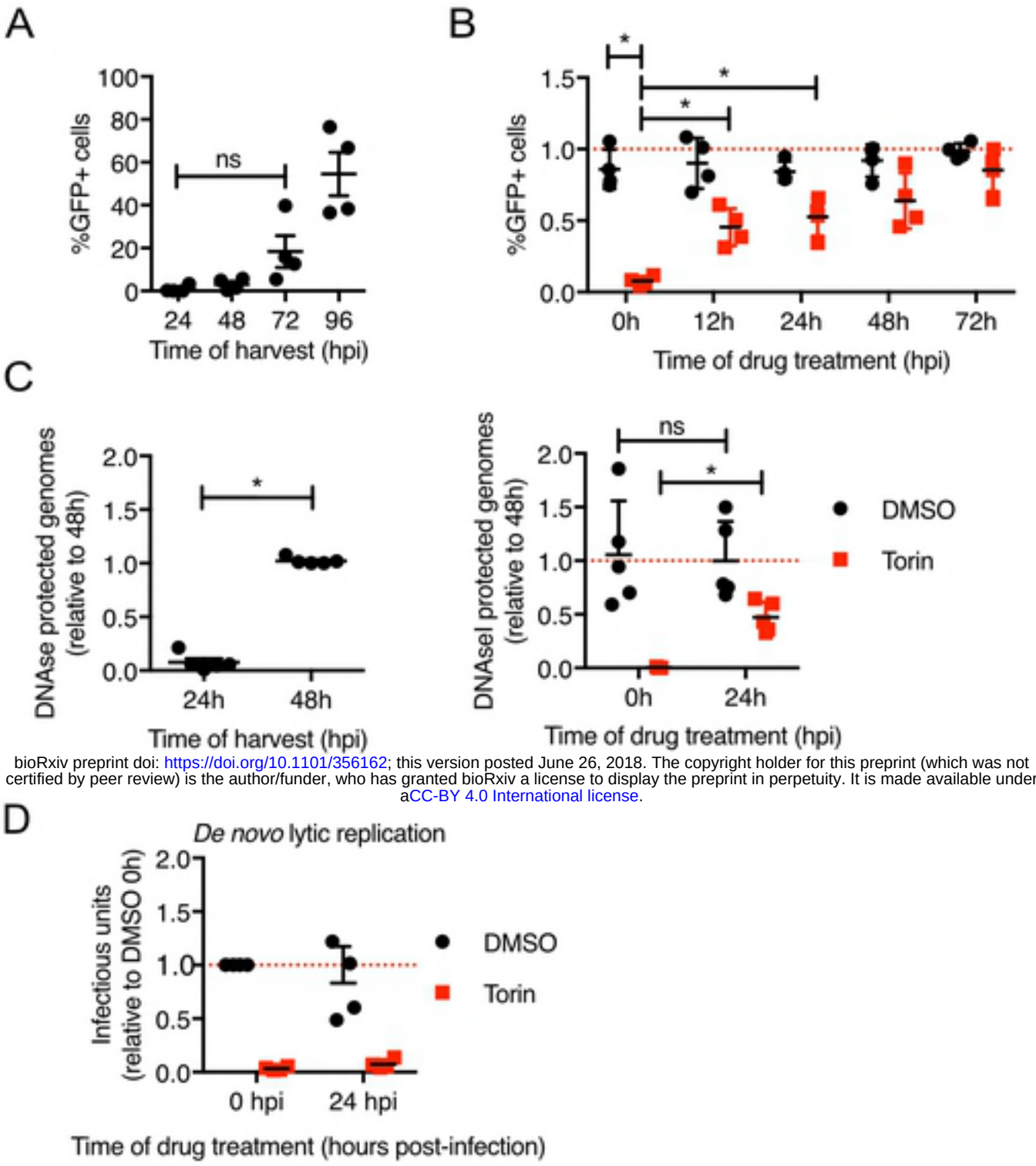

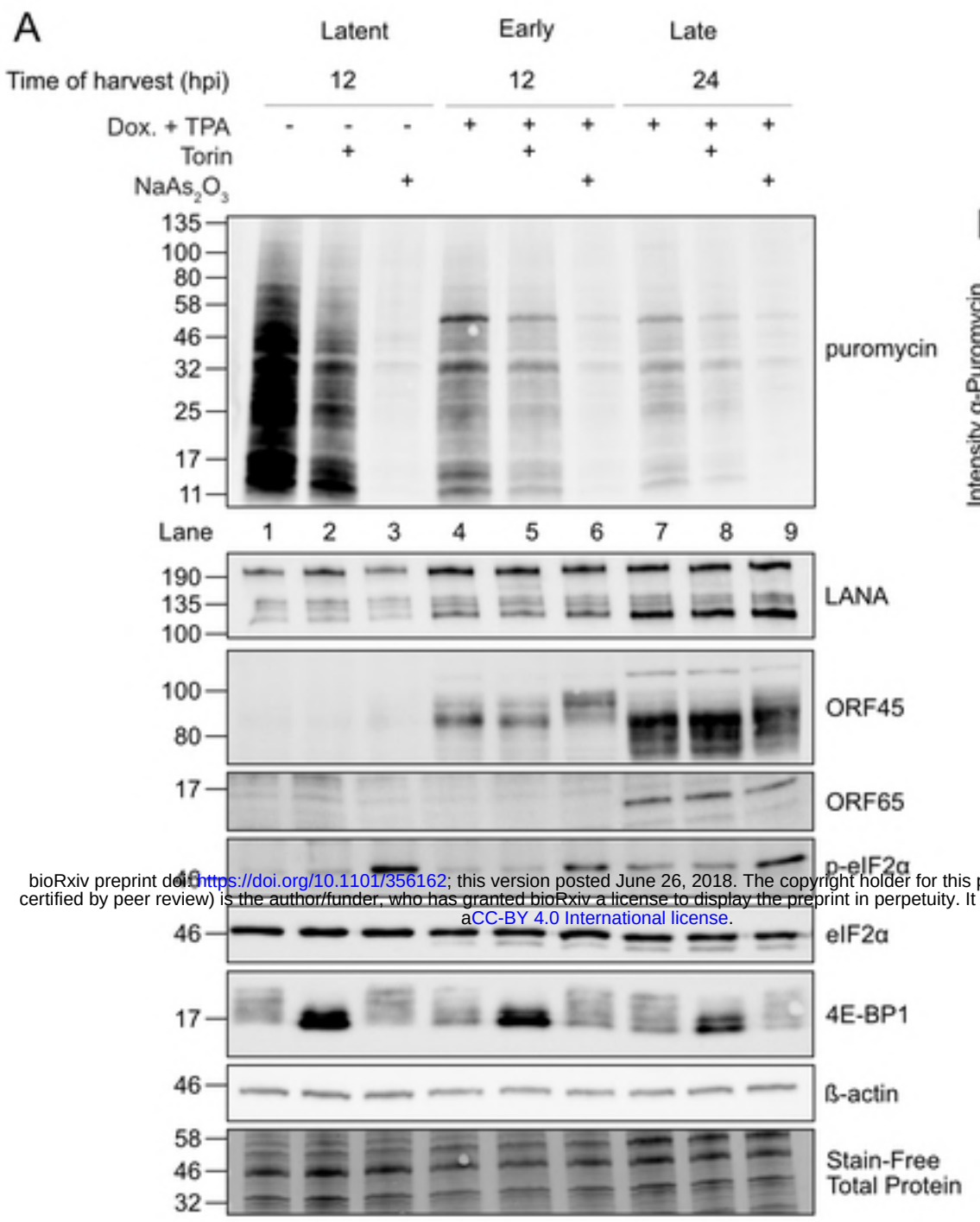

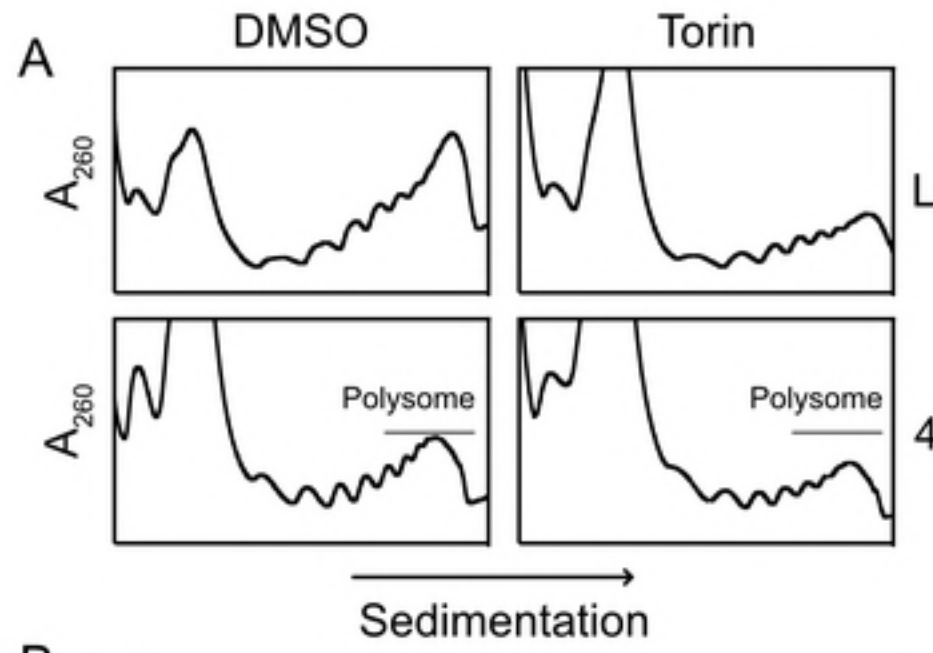

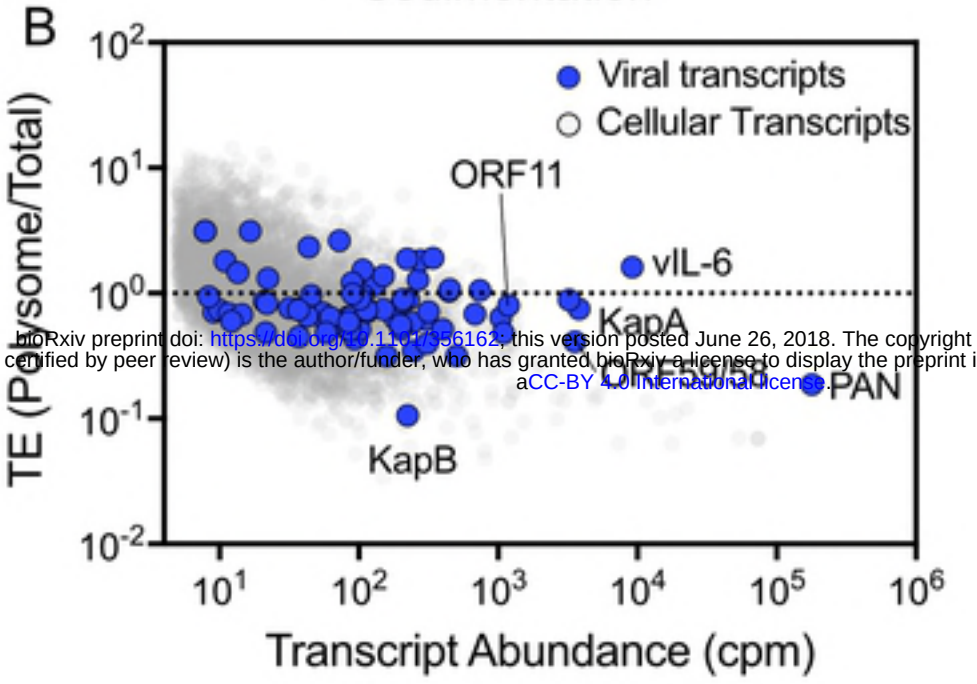

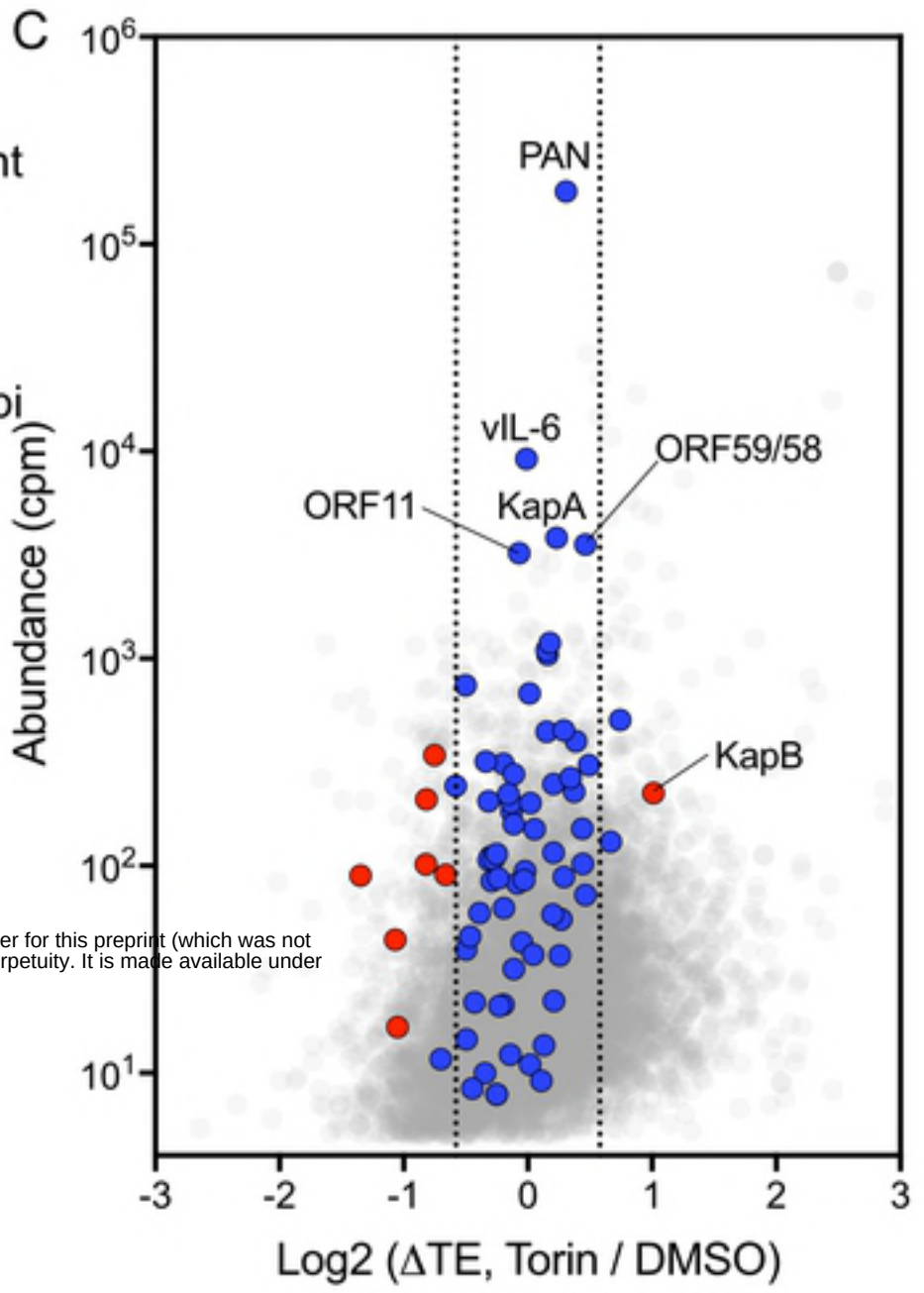

Cellular Transcripts
Virus Transcipts (Z > 1 or Z < -1)
Virus Transcripts (-1 < Z < 1)